Use of CFRP Overlays to Strengthen Welded Connections under Fatigue Loading

Fatih Alemdar[1]; Adolfo Matamoros[2]; Caroline Bennett, M.ASCE[3]; Ronald Barrett-Gonzalez[4]; and Stanley T. Rolfe, F.ASCE, Hon.M.ASCE[5]

Abstract: This study evaluates the performance of various methods to prevent and repair fatigue damage in welded connections, a recurring problem that affects a significant number of steel bridges. Experimental tests and analytical simulations were carried out to investigate the fatigue performance of coverplate specimens in which the welded connections were reinforced with carbon-fiber reinforced polymer (CFRP) overlays. Specimens were loaded in three-point bending induced by a cyclic load to evaluate the change in fatigue-crack initiation life of the welded connections caused by the attachment of the CFRP overlays. Test results showed that when bond between the CFRP overlays and the steel was maintained, the reduction in stress demand was sufficient to extend the fatigue life of the welded connections from AASHTO fatigue-design Category E' in the unreinforced configuration to the infinite fatigue life range. Test results also showed that the fatigue strength of the bond layer was drastically improved by introducing breather-cloth material within the bond layer. **DOI: 10.1061/(ASCE)BE.1943-5592.0000230.**

CE Database subject headings: Fatigue; Composite materials; Rehabilitation; Welded connections; Steel bridges.

Author keywords: Fatigue; CFRP; Composite; Retrofit; Welded connections; Steel bridge; Resin.

Introduction

A significant number of studies have been performed, mostly in the aerospace field, to investigate the use of Fiber Reinforced Polymers (FRPs) to repair metal plates with fully developed fatigue cracks (i.e., Sabelkin et al. 2007; Schubbe et al. 1999; Tavakkolizadeh et al. 2003). In most instances found in literature, preexisting cracks or notches were covered with one or a few layers of composite sheets to effectively reduce the rate of crack growth. Very few studies (Nakamura et al. 2009) have investigated the use of composite materials to repair or strengthen welded connections. Because welded connections are quite common in existing bridge structures, and because the implementation of repairs in this type of connection is often challenging because of limitations imposed by complex geometry, the use of composite materials presents a new alternative that expands the tools available to bridge engineers.

In terms of linear elastic fracture mechanics theory, there are essentially three alternatives to improve fatigue life, if material properties remain the same (Barsom et al. 1999): (1) reduce the initial flaw size, (2) reduce the stress range, or (3) induce a residual stress field that will cause the area subjected to fatigue loading to be in compression.

Repair methods such as laser peening and ultrasonic impact treatment improve fatigue life by reducing the initial flaw size and introducing a residual stress field. Other repair techniques, such as bolting and attachment of fiber reinforced polymer (FRP) overlays, increase fatigue life by reducing the stress demand. Many examples are available in the literature that show the effectiveness of FRP materials when used to repair existing notches or cracks. For example, Tavakkolizadeh et al. (2003) concluded that the use of FRP sheets to repair notched beam flanges led to significant improvements in fatigue life. Because FRP repairs work by reducing the stress range experienced in the metal substrate, this method should be effective before and after crack initiation, as long as the bond between the FRP and the underlying metal is maintained.

The focus of the present study builds on work performed by Kaan (2008) and Vilhauer et al. (2012) by examining the effectiveness of various configurations of FRP overlays, and comparing their performance with other methods of fatigue retrofitting, including ultrasonic impact treatment and weld grinding. Two types of FRP overlays are considered in the present work: those made using conventional lay-up techniques, and those created using a spray-on method (chopped fiber overlays). Parameters influencing the performance of the overlays are given significant attention in the present work, such as geometric properties of the overlay, modulus of elasticity of the FRP, thickness of the resin layer used to attach the FRP overlay to the steel surface, and the presence of an unbonded region (gap) in the direct vicinity of the weld. Finally, in the present work, fatigue life of the bond layer between the FRP overlays and the substrate is closely differentiated from the fatigue life of the retrofitted steel specimens.

Background

Several studies conducted in the past (Nakamura et al. 2009; Tavakkolizadeh et al. 2003), including recent experimental work

[1]Graduate Research Assistant, Univ. of Kansas, 1530 W. 15th St., Lawrence, KS 66045. E-mail: alemdar@ku.edu

[2]Associate Professor, Univ. of Kansas, 1530 W. 15th St., Lawrence, KS 66045 (corresponding author). E-mail: abm@ku.edu

[3]Assistant Professor, Univ. of Kansas, 1530 W. 15th St., Lawrence, KS 66045. E-mail: crb@ku.edu

[4]Associate Professor, Univ. of Kansas, 1530 W. 15th St., Lawrence, KS 66045. E-mail: barrettr@ku.edu

[5]Learned Professor, Univ. of Kansas, 1530 W. 15th St., Lawrence, KS 66045. E-mail: srolfe@ku.edu

Note. This manuscript was submitted on October 4, 2010; approved on February 9, 2011; published online on July 22, 2011. Discussion period open until October 1, 2012; separate discussions must be submitted for individual papers. This paper is part of the ***Journal of Bridge Engineering***, Vol. 17, No. 3, May 1, 2012. ©ASCE, ISSN 1084-0702/2012/3-420–431/$25.00.

from a related study on welded steel connections (Kaan 2008), show that bonding FRP sheets or overlays can be a very effective technique to improve fatigue-crack initiation life and fatigue-crack propagation life in steel bridge components. This study focuses on the repair of welded cover plate connections that have thick cover plates, which are known to be vulnerable to fatigue damage (Albrecht et al. 2007), using prefabricated Carbon-Fiber Reinforced Polymer (CFRP) overlays. This particular type of connection was chosen because its geometry falls within the worst fatigue category in the AASHTO LRFD Bridge Design Specification (2004), Category E', and consequently allows for the evaluation of strengthening techniques that bring about large increases in fatigue life.

A thorough review of experimental work carried out to characterize the fatigue performance of welded cover plates in steel beams, including several retrofit techniques, is presented by Albrecht et al. (2007). Experimental data presented in their review showed that three techniques—end bolting, splicing, and bonding of the cover plates with an epoxy adhesive—resulted in large increases in fatigue-life, pushing the beams to the infinite fatigue-life range.

The present study is a continuation of studies carried out by Vilhauer et al. (2012), Petri (2008), and Kaan (2008), evaluating the performance of various repair and retrofit measures for welded connections. Vilhauer et al. (2012) tested 17 steel-welded cover plate specimens (Fig. 1) to investigate the performance of several fatigue strengthening methods. The specimens used by Vilhauer (which had the same dimensions as those used in this study) consisted of two steel plates connected all around with an 8-mm (5/16-in.) shielded metal arc (SMAW) fillet weld. One plate had dimensions of $1{,}270 \times 114 \times 25$ mm ($50 \times 4.5 \times 1.0$ in), whereas the other had dimensions of $660 \times 76 \times 25$ mm ($26 \times 3.0 \times 1.0$ in.). Both plates were Grade A36 steel. The specimen was supported in the vertical direction at a distance of 76 mm (3.0 in.) from both edges of the larger plate. Vilhauer et al. (2012) evaluated three different fatigue strengthening methods: ultrasonic impact treatment (UIT), a post-installed fully tensioned structural high-strength bolt, and a combination of the two techniques. Vilhauer et al. (2012) found that specimens in which the welds were treated with UIT were able to reach infinite fatigue life when tested at a stress range of 138 MPa (20 ksi).

Kaan (2008) studied the use of CFRP overlays for increasing fatigue-crack initiation life (Fig. 2). Kaan (2008) conducted experiments with two different types of prefabricated overlays: Type I and Type II. Type I overlays were fabricated by placing successive layers of bidirectional woven carbon-fiber ply until the desired geometry was achieved. Type II overlays [Fig. 2(b)] were developed to obtain greater consolidation and uniformity than achieved in Type I overlay elements. Type II overlays were comprised of 36 plies of bidirectional woven carbon fiber plies (pre-impregnated with cyanamide-123 resin) and 4 plies of boron fiber. In testing the Type I overlays, fatigue failure occurred through the composite material, instead of the bond layer or the welded connection.

The results of multiple test trials carried out by Kaan (2008) on four different fatigue specimens reinforced with Type II CFRP overlays are presented in Table 1. Although the test results showed that the fatigue-crack initiation life of the welded connections increased when the specimens were reinforced with CFRP overlays, repeated bond failures between the CFRP and the steel occurred. When debonding of the overlay occurred, the specimen was subjected to fatigue cycles in the unreinforced configuration until debonding was noticed through inspection; in these cases, the CFRP overlay was reattached to the steel specimen after subsequent inspection for cracks. After multiple debonding failures, the steel substrate was subjected to a significant number of load cycles in the unreinforced configuration, placing it at greater risk for developing a fatigue crack. For this reason, these tests provided meaningful information about the effect of the interface layer configuration on the bond life under fatigue loading, and also showed that use of the overlays led to an increase in the fatigue-crack initiation life of the welded connections; however, the tests did not present an appropriate measure of the magnitude of the increase in fatigue life of the welded connection when bond between the CFRP overlay and the steel substrate is maintained throughout the test.

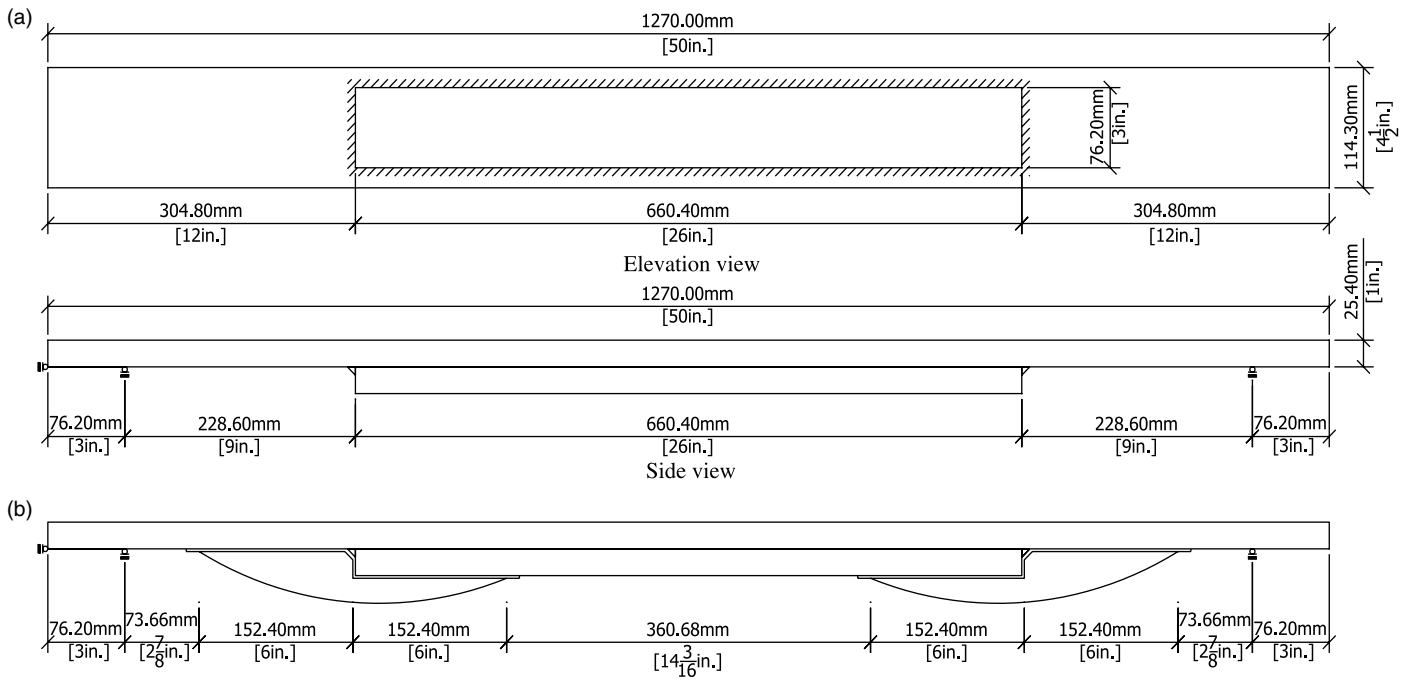

Fig. 1. Three-point bending specimens: (a) without CFRP retrofit [adapted from Vilhauer et al. (2012)]; (b) with CFRP retrofit applied [adapted from Kaan (2008)]

J. Bridge Eng. 2012.17:420-431.

Table 1. Experimental Results of Three-Point Bending Tests Performed by Kaan (2008) and Vilhauer et al. (2012)

Type of treatment	Specimen design	Resin thickness, mm (in.)	Duration of test (No. of cycles)	No. of cycles to crack initiation	Average no. of cycles to CFRP debonding	No. of debonds	Reference
CFRP	TRI 02	0.76 (0.030)	900,000	460,000	588,000	2	Kaan (2008)
CFRP	TRI 06	1.65 (0.065)	1,554,656	N/A	431,500	5	Kaan (2008)
CFRP	TRI 04	3.18 (0.125)	2,051,800	1,329,800	239,070	6	Kaan (2008)
CFRP	TRI 05	6.35 (0.250)	1,634,756	N/A	1,205,000	1	Kaan (2008)
None	Cntrl_03			500,000			Vilhauer et al. (2012)
None	Cntrl_05			350,000			Vilhauer et al. (2012)
UIT	Uit_02			5,000,000			Vilhauer et al. (2012)

Note: All specimens tested at a stress range of 138 MPa (20 ksi).

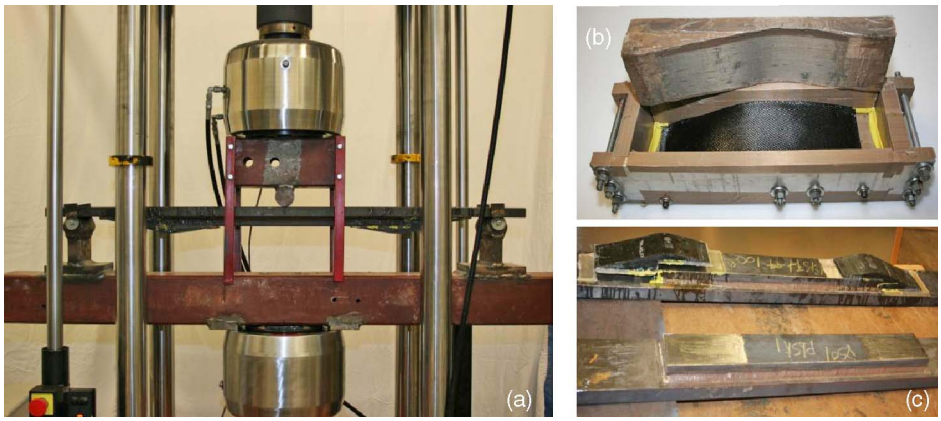

Fig. 2. Three-point bending specimens: (a) test setup; (b) CFRP overlay in fabrication mold; (c) unreinforced and reinforced specimens side by side

The two main conclusions from the tests performed by Kaan (2008) were that the use of CFRP overlays led to a significant increase in fatigue-crack initiation life of the welded connections, and that maintaining the bond between the CFRP and the steel substrate was a critical factor in achieving the largest possible increase in fatigue-crack initiation life.

Objective

The primary objective of this study was to investigate the effectiveness of CFRP overlays as a fatigue-strengthening method (attaching overlays before crack initiation) for welded connections, and to compare its effectiveness with that of other methods used to strengthen welded connections. The second objective was to determine the effectiveness of CFRP overlays in reducing the fatigue-crack propagation rate when used as a repair method (attaching overlays after crack initiation).

To meet both objectives, three-point bending welded cover plate specimens were tested in fatigue under a constant stress range. Prefabricated CFRP overlays were bonded to the ends of the cover plates both before loading and after fatigue cracks were observed in the welds.

To complement the experimental study, a suite of finite-element analyses were performed to characterize the stress field in the region surrounding the weld toe, and to quantify the effect of the characteristics of the overlay on the stress demand.

Finite-Element Simulations

The stress distribution in specimens tested by Vilhauer et al. (2012) and Kaan (2008) was studied by Petri (2008) with 3D analyses performed using the finite-element software ABAQUS V.6.8 (Simulia 2008). Models were created using linear elastic material models for the steel and composite materials, and a mesh consisting of 20-node brick elements. The interface between the two plates was modeled as a contact surface, and analyses were performed with various assumptions about the interaction between the plates, ranging from a frictionless surface to a fully attached surface. The welds were modeled as separate parts and rigidly connected to the plates using the tie constraint technique in ABAQUS (Simulia 2008). The analyses showed that attaching CFRP overlays to a welded steel cover plate connection would result in a significant reduction of peak stress at the toe of weld, which was consistent with the increase in fatigue life observed experimentally by Kaan (2008).

Deflected shapes and computed maximum principal stresses under the peak load from the various computational models analyzed by Petri are shown in Fig. 3. The stress fields show that the composite overlays were effective in reducing the high stress demands that occurred at the weld toe of the unreinforced specimen, and in distributing those stresses over a much greater area. A comparison of Figs. 3(b)–3(d) shows that there was a spike in stress field near the edge of the CFRP overlay closest to the end of the specimen, and that the magnitude of the spike decreased as the length of the overlay increased. Because of the spike in the stress field, this point is of critical importance in maintaining the bond between the FRP overlay and the substrate steel, particularly in the case of shorter overlays. Additional finite-element simulations were conducted as part of this study. Two-dimensional (2D) finite-element models were developed in ABAQUS v.6.8.2 (Simulia 2008) using linear elastic material properties and 4-node plane strain elements. The 2D model captured a 25-mm (1-in.) mid-width strip of the specimen. Twenty different models were

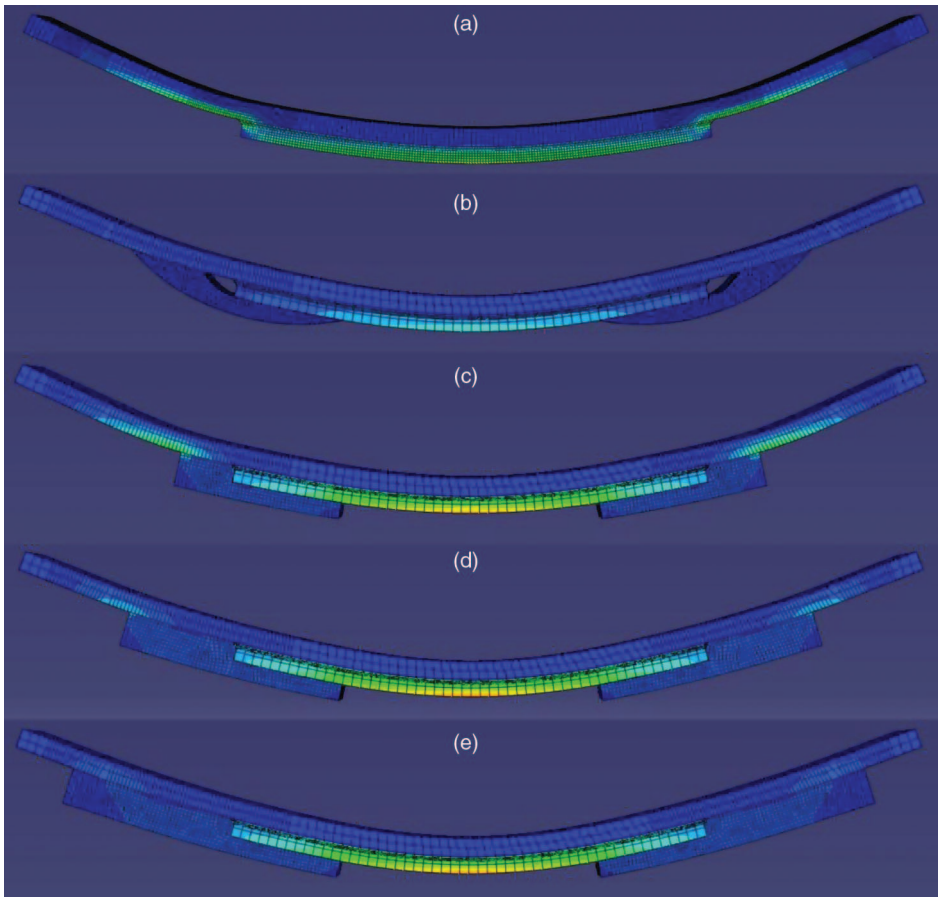

Fig. 3. (Color) Elevation view showing maximum principal stress: (a) control specimen; (b) specimen with smooth-shaped composite overlay; (c) short rectilinear composite overlay; (d) rectilinear composite overlay; (e) long rectilinear composite overlay

analyzed to provide the basis for a parametric study. Parameters investigated included the geometric profile of the overlay, its length, thickness (Fig. 4), modulus of elasticity of the CFRP, thickness of the resin layer used to attach the CFRP overlay to the steel surface, and the presence of an unbonded region (gap) in the direct vicinity of the weld. Each parameter was varied while the others remained constant. The reference values for the modulus of elasticity of the composite and the thickness of the resin layer were 26.5 GPa (3850 ksi) and 6 mm (1/4 in.), respectively, and the modulus of elasticity of the resin was 3.5 GPa (500 ksi). The different geometric profile parameters that were investigated are shown in Fig. 4.

The parametric study was intended to determine the optimum configuration of the CFRP overlay and to investigate how effective the overlay would be in decreasing the peak-stress demand at the weld toe. Computed stress fields in the vicinity of the weld for

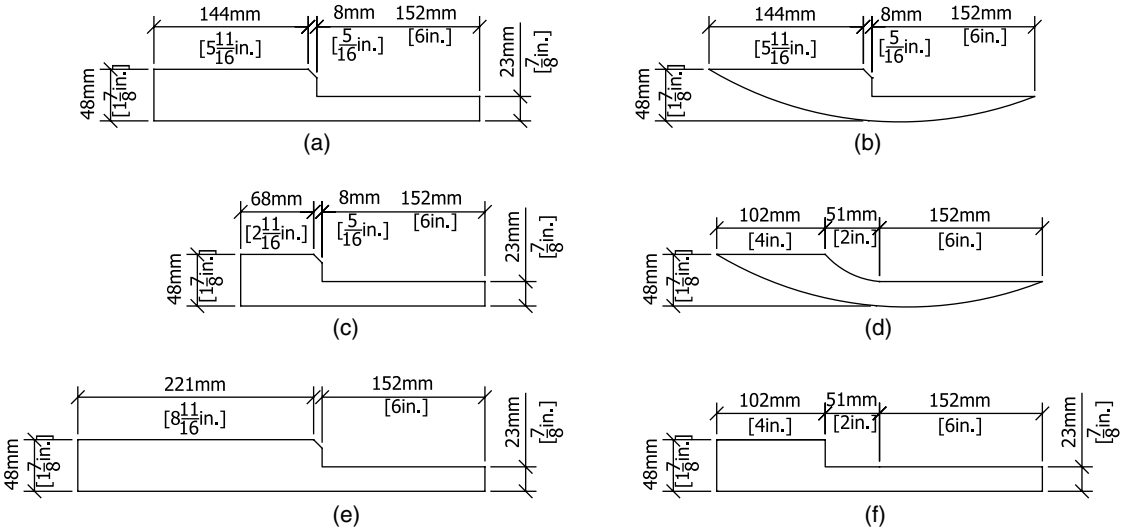

Fig. 4. Configuration of CFRP overlays evaluated in the analytical model

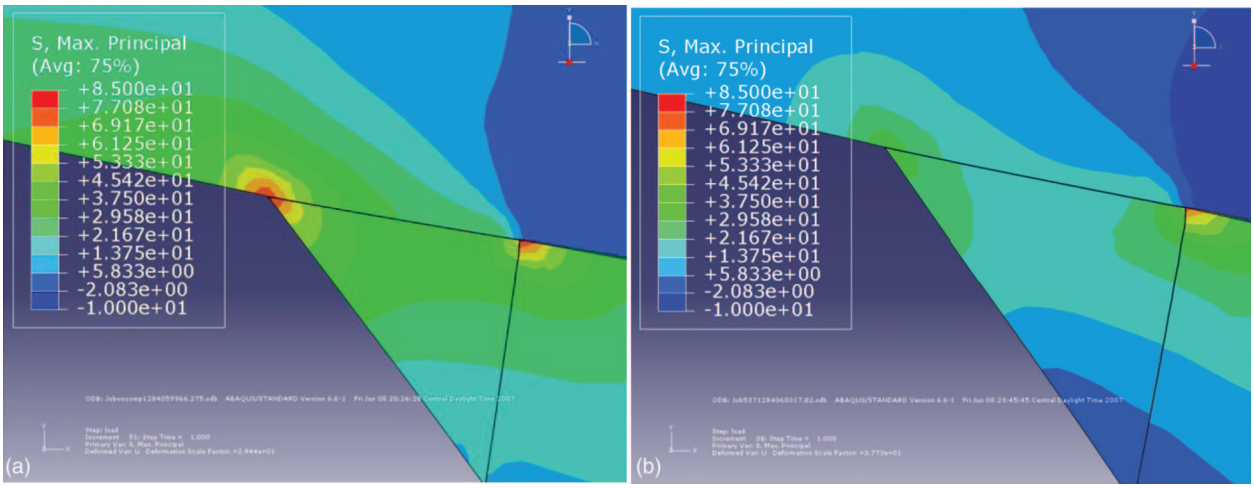

Fig. 5. (Color) Elevation view showing maximum principal stress: (a) control specimen; (b) specimen with smooth-shaped composite overlay (overlay not shown for better clarity)

the unreinforced and reinforced [Fig. 4(b)] configurations are presented in Fig. 5. The 2D simulation results were consistent with those obtained by Petri (2008) in that the addition of the overlay resulted in a significant reduction in the peak-stress demand at the weld toe [approximately 80% for the overlay configuration shown in Fig. 4(d)]. These simulation results were also consistent with the increments in fatigue-life increase observed by Kaan (2008).

The finite-element analyses also showed that the reduction in the maximum principal stress was not as significant at the root of the weld as it was at the toe of the weld. Unreinforced specimens, in which cracks were allowed to propagate until structural failure of the specimen, exhibited crack initiation at the toe of the weld, consistent with the computed stress field for the unreinforced configuration shown in Fig. 5. In the case of reinforced specimens, tests conducted by Kaan in which debonding took place showed that the fatigue behavior after debonding was similar to that of unreinforced specimens, with cracks initiating at the toe of the weld and propagating through the plate from that location. In specimens in which debonding of the overlays did not take place, the specimens did not develop visible cracks by the time the infinite fatigue-life range was reached. Given the configuration of the specimens it was not possible to inspect the back of the welds for cracks, so the only conclusion that could be drawn about the behavior at the root of the weld was that either the reduction in stress demand at the root of the weld was sufficient to achieve infinite fatigue-life, or that if fatigue cracks developed at this location, the reduction in the stress demand was sufficient to delay the propagation of those cracks so that there were no visible signs of damage or measurable changes in the stiffness in the specimens when the infinite fatigue-life range was achieved.

The suite of finite-element simulations performed in this study evaluated the effect of the following parameters: geometric configuration of the overlay, thickness of the interface bond layer, and the modulus of elasticity of the composite. The 2D simulations showed that the geometric profile of the CFRP overlay did not have a significant effect on the calculated stress demand at the weld toe, whereas the presence of a gap between the weld and the CFRP overlay did have a notable effect. This is illustrated in Figs. 6 and 7, which present the computed longitudinal stress along a path on the surface of the bottom steel plate. The observed trends in the calculated longitudinal stress and the maximum principal stress were similar in nature, so the directional stress presented in the figures was chosen on the basis of clarity.

In Figs. 6 and 7 the spike in stress observed at a distance of approximately 298 mm (11.8 in.) from the edge of the specimen corresponds to the location of the toe of the weld, whereas the root of the weld was located at approximately 307 mm (12.1 in.) from the edge of the specimen. The distance from the edge of the specimen shown in the two figures corresponds to the "true distance" measured in the computed deformed configuration. This causes a slight offset in the locations of the toe of the weld and the root of the weld in the curves shown in Figs. 6 and 7. Results were plotted using this coordinate system to facilitate observing similarities and differences among the curves.

Fig. 6. shows that a curved and a rectilinear CFRP overlay configuration were equally effective in reducing the peak-stress demand at the toe of the weld. Fig. 7. shows that the most effective retrofit scheme involved bonding the overlay up to the location of the weld, which resulted in a reduction on the peak-stress demand at the weld toe of approximately 80%. When the analysis was performed leaving a gap near the weld toe [configuration shown in Fig. 4(d)] the reduction in peak-stress demand at the weld toe was still very significant, approximately 60%, but the efficiency of the repair was diminished. The analyses showed that within the evaluated range of values, other parameters related to the shape of the CFRP overlay, such as length and the thickness of the overlay, did not significantly affect stress demand at the toe of the weld.

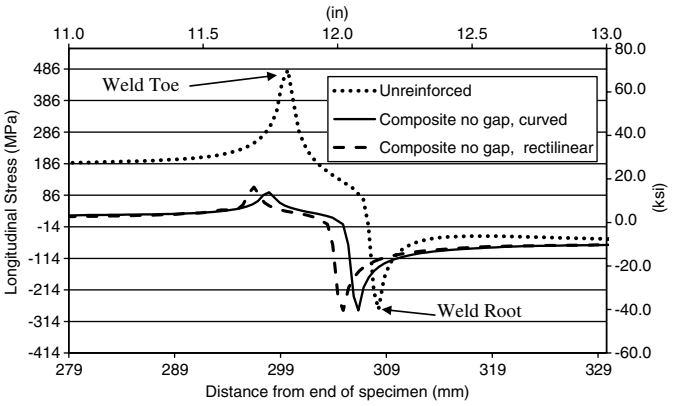

Fig. 6. Effect of composite overlay shape on longitudinal stresses in area of weld

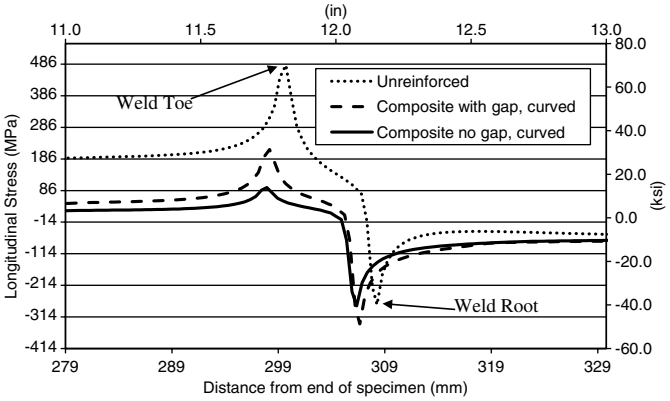

Fig. 7. Effect of presence of an unbounded gap over weld on longitudinal stresses in area of weld

Of the remaining parameters, the modulus of elasticity of the composite and the thickness of the interface bond layer had the most significant effect on the stress demand at the weld toe. The effect of the modulus of elasticity of the CFRP overlay is illustrated in Fig. 8. A reference value of 26.6 GPa (3,860 ksi) was adopted for the modulus of elasticity on the basis of experimental measurements performed on the composite material used to fabricate the overlays used in this study. A suite of FE analyses were performed in which the CFRP modulus of elasticity ranged between 60% of the reference value (16 GPa [2,315 ksi]) and 400% of the reference value (106 GPa [15,430 ksi]). Results presented in Fig. 8 are for the overlay configuration shown in Fig. 4(b). Fig. 8 shows that equal successive increments in the modulus of elasticity of the CFRP overlay resulted in decreases in stress demand. These results suggest that prefabricating the overlay to achieve higher fiber contents, as was done in this study, improves the effect of the repair on the fatigue life of the welded connection. The results also suggest that, for the analyzed overlay configurations, paying a premium for very stiff fibers may not bring about a meaningful increase in fatigue life beyond that achievable with conventional fibers.

The effect of the thickness of the interface layer is illustrated in Fig. 9, which shows that explicitly modeling the flexibility of the interface layer resulted in a lower stress demand at the weld toe, likely because of the effects of bending on the overlays. When the interface layer was modeled, increasing the thickness of the overlay resulted in a slight increase in the peak-stress demand at the weld toe. This indicates that a thicker interface layer is less effective in reducing the peak-stress demand at the weld toe than a thinner interface layer. However, the analyses also showed that

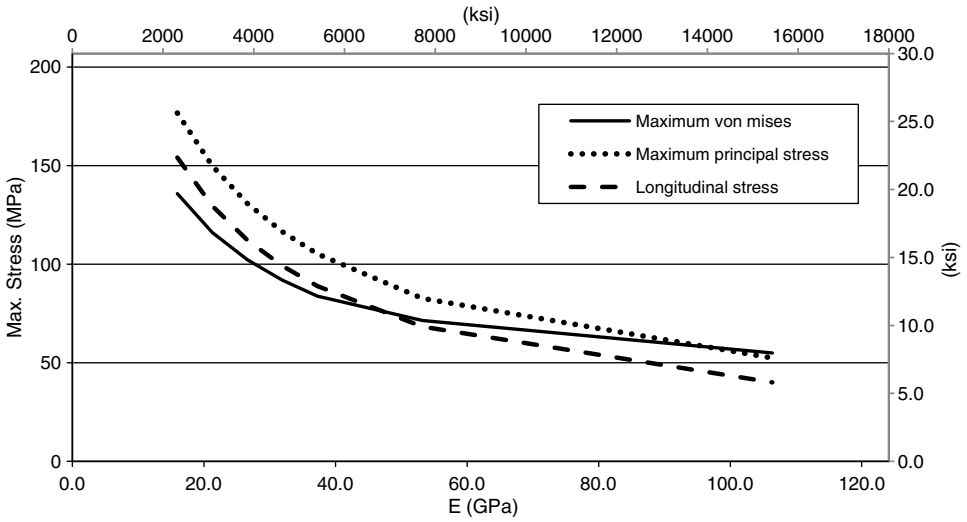

Fig. 8. Effect of composite overlay stiffness on maximum stress demand at weld toe

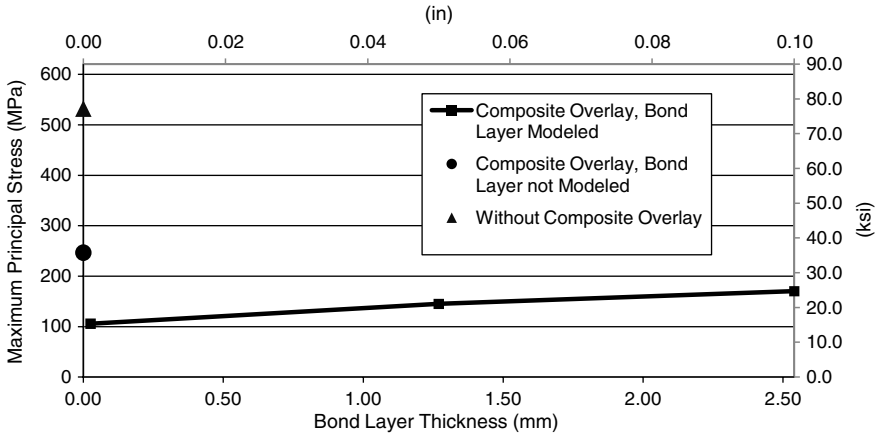

Fig. 9. Maximum principal stress on steel plate in vicinity of weld as a function of thickness of bond layer

J. Bridge Eng. 2012.17:420-431.

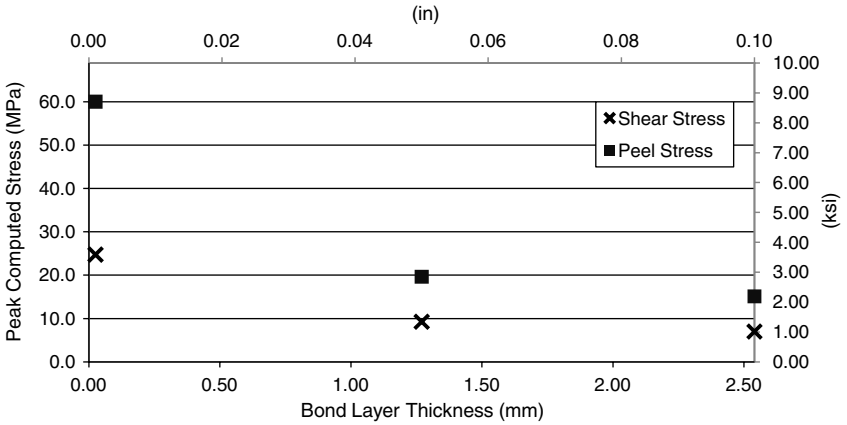

Fig. 10. Maximum computed stress at interface between composite and bond layer

peak-shear and peel-stress demands at the interface between the composite and the bond layer exhibited the opposite trend. Fig. 10 shows that as the thickness of the interface decreased (which reduces the calculated stress demand at the weld toe), both the calculated peak-shear and peel-stress demands increased, which can be expected to have a detrimental effect on bond strength under cyclic loading.

Experimental Analysis

The experimental program consisted of a series of welded cover plate specimens loaded in three-point bending and subjected to cyclic loading under a constant stress range (Figs. 1 and 2). The three-point bending specimens consisted of two plates with identical dimensions as those studied by Vilhauer et al. (2012) and Kaan (2008), and previously described in the background section. The specimens were restrained from vertical motion at points 76 mm (3.0 in.) from the edges of the larger plate. The smaller plate was attached to the larger plate with a continuous 8-mm (5/16-in.) fillet weld all around the perimeter of the smaller plate. The effect of weld imperfections on the fatigue performance of the repair methods was not a parameter investigated in the study. An effort was made to ensure that all welds in the specimens were similar in nature by having all welding performed by the same fabricator using the same technique under similar conditions. The welds were of good quality with no visible signs of undercut at the toe of the weld and had a slightly convex profile.

The experimental matrix is summarized in Table 2. As shown, three different types of treatments were used, including three different types of composite overlays. To establish a frame of reference on the basis of the type of geometric discontinuity, the welded connection between the two plates was classified as an AASHTO Category E' detail (AASHTO 2004). According to the AASHTO design curves, the nominal stress range for a Category E' detail should be maintained below 31.0 MPa (4.5 ksi) in the area of the weld to ensure that cracking will not initiate under fatigue loading. Loads were selected to achieve a high stress range of 138 MPa (20.0 ksi) at the transverse welds, at the location of the weld toes. The ratio of maximum to minimum load was selected as $R = 0.1$. The maximum load was 17.1 kN (3.84 kips) and the minimum load was 1.7 kN (0.38 kips).

Three specimens were strengthened with prefabricated multilayered CFRP overlays, and were designated as TRI 04, TRI 06, and TRI 07. Multilayered CFRP overlays were prefabricated following the same procedure used by Kaan (2008) for Type II

Table 2. Experimental Matrix

Specimen ID	Stress range MPa (ksi)	Thickness of bond layer[a] mm (in.)	Treatment type	Fiber type
TRI 04	138 (20)	6.4 (0.25)	CFRP overlay	Carbon
TRI 06	138 (20)	6.4 (0.25)	CFRP overlay	Carbon
TRI 07	138 (20)	3.2 (0.25)	CFRP overlay	Carbon
CHP1	138 (20)	None	Chopped fiber	Carbon
CHP2	138 (20)	6.4 (0.25)	Chopped fiber	Carbon
CHP3	138 (20)	6.4 (0.25)	Chopped fiber	Glass
GRND 1	193 (28)		Smoothed weld	
GRND 2	193 (28)		Smoothed weld	
GRND 3	193 (28)		Smoothed weld	
GRND 4	193 (28)		Smoothed weld	
Control (TRI 08)	138 (20)			

[a]When multiple bond-layer configurations were used in the same specimen, the value shown is for configuration with breather cloth.

overlays. The dimensions of CFRP overlay were $300 \times 76 \times 38$ mm ($12 \times 3.0 \times 1.5$ in.). The shape of CFRP was curved in profile, without leaving any gap between weld and the CFRP [Fig. 4(b)]. Breather cloth approximately 2-mm (0.1-in.) thick was embedded within the resin layer to improve bond behavior under cyclic loading.

Of the three specimens treated with mulilayered CFRP overlays, two (TRI 06 and TRI 07) were intended to study the effectiveness of CFRP overlays for preventing fatigue damage in the area near the weld toe. The remaining specimen (TRI 04) was used to investigate the effectiveness of the CFRP overlays to repair a connection with a pre-existing fatigue crack in the weld. One of the uncracked specimens (TRI 07) had never been loaded before, whereas the other two specimens (TRI 04 and TRI 06) had already been subjected to fatigue loading by Kaan (2008).

In addition to the specimens described previously, three specimens were treated with chopped-fiber overlays. The chopped-fiber overlays were fabricated using an external mixing spray machine (a nonatomized resin LEL chopper system commercialized by BINKS). The spray machine used a vinyl ester resin with Norox MEKP-925 catalyst and graphite fiber yarn. Before spraying the composite material, the surface of the steel substrate was abraded using an angle grinder and cleaned with acetone and isopropyl alcohol. After cleaning, the fiber-resin mix was sprayed in layers approximately 3-mm (1/8-in.) thick and compacted using a hand tool. Overlay CHP 1 had the configuration shown in Fig. 4(a),

Fig. 11. (Color) Composite overlays used in the study

whereas the shape of overlays CHP 2 and CHP 3 was similar to that of the prefabricated multilayered CFRP overlay [Fig. 4(b)]. All overlays used in the testing program are shown in Fig. 11. After spraying was completed, the specimen was cured at room temperature for 2 days, after which the remnant resin was cleaned from the steel substrate. In the specimen designated CHP 2, a breather cloth layer was placed on the surface of the steel and saturated with resin before spraying the combined resin-chopped graphite-fiber mix. In the specimen designated CHP 3, the breather cloth was soaked with Hysol® resin and cured for 2 h at room temperature before a resin-chopped glass-fiber mix was sprayed.

All other specimens tested were not treated with composite overlays. An additional control test (TRI 8) was performed to complement the data set developed by Vilhauer et al. (2012) on identical specimens (Table 1). The remaining specimens without overlays (GRND 1 through GRND 4) were treated by smoothing out the roughness of the surface of the welds using an angle grinder. When the smoothing process was finished, the surface of the weld was relatively flat, and formed an angle of approximately 45° with respect to the surface of both plates. After grinding, the surface of the weld was cleaned with a steel brush to ensure imperfections from the welding process had been removed. This process was repeated until no imperfections were visible. The two goals of the weld treatment were to ensure that there was a smooth transition between the weld and the plate at the weld toe, and to significantly reduce the initial size of the weld flaws created during the welding process.

Measured material properties are presented in Table 3. Coupon tests performed in accordance with ASTM 3039/D 3039M (ASTM 2000) from single-layered specimens showed that the modulus of elasticity of the CFRP was approximately 83 GPa (12,000 ksi). The modulus of elasticity of the 9412 Hysol® resin and of the chopped fiber composite were also measured using coupon tests (Table 3) as prescribed by ASTM 3039/D 3039M (ASTM 2000). The measured modulus of elasticity of the resin was 2.1 GPa (300 ksi). The yield strength of the steel was found to be 300 MPa (43 ksi), and the tensile strength was 490 MPa (71 ksi).

Results from Three-Point Bending Specimens under Fatigue Loading

Two common modes of fatigue failure were observed in the tests carried out by Vilhauer et al. (2012), Kaan (2008), and those performed as part of this study: fatigue failure of the bond layer between the composite and the steel, and fatigue failure of the welded connection. For this reason, the results are interpreted in terms of two different types of fatigue tests: those related to the fatigue life of the bond layer (Table 4), and those related to the fatigue life of the welded connection (Table 5).

Debonding of the overlay under fatigue loading occurred in a relatively rapid manner (Kaan 2008). Bond layers were periodically examined by visual inspection and by monitoring the stiffness of the specimen computed on the basis of the applied load and the vertical displacement at the center. Failure of the bond layer typically initiated at the edge of the overlay closest to the end of the specimen and propagated through the bond layer toward the toe of the weld (Kaan 2008). Welds were inspected for the presence of cracks with dye penetrant using the technique adopted by Vilhauer et al. (2012). Cracks typically initiated at the weld toe, near the center of the weld, and propagated toward the edge of the specimen.

Fatigue Strength of the Bond Layer

The study by Kaan (2008) showed that composite overlays can effectively prevent fatigue failure of the welded connection, but to do so, it is essential to avoid failure of the bond layer resulting from fatigue. The effects of various bonding techniques on the fatigue strength of the bond layer are shown in Fig. 12, and test results are summarized in Table 4. Designations for the experiments carried with multilayered CFRP overlays were defined in terms of the thickness of the bond layer. In specimens in which multiple bond failures took place, the overlay was reattached to the same cover plate specimen after each failure event. Overlays were inspected and reused if undamaged. Specimens without breather cloth and resin pool [tested by Kaan (2008)] are designated by the letter C, specimens with a resin pool extending beyond the edge of the overlay (Kaan 2008) are designated by the letters CP, those

Table 3. Material Test Results

Material		Coupon thickness mm (in.)	Number of coupons	Average modulus of elasticity GPa (ksi)	Standard deviation GPa (ksi)
CFRP	1 Layer	0.30 (0.012)	3	85.8 (12,438)	10.0 (1,445)
	3 Layers	1.02 (0.040)	4	75.3 (10,926)	10.9 (1,581)
	5 Layers	1.98 (0.078)	3	61.7 (8,944)	0.3 (42)
9412 Hysol® resin		6.4 (0.25)	6	2.1 (303)	0.2 (25)
Chopped fiber (graphite fiber)		4.8 (0.19)	7	14.1 (2,052)	6 (866)
Chopped fiber (glass fiber)		5.6 (0.22)	1	1.4 (202)	—

Note: All coupons had a width of approximately 1 in.

J. Bridge Eng. 2012.17:420-431.

Table 4. Fatigue Life of Bond Layer for Various Bonding Techniques

Test designation	Resin layer thickness, mm (in.)	Number of cycles to bond failure[a]
C0030-01	0.76 (0.03)	275,000
C0030-02	0.76 (0.03)	900,000
C0125-01	3.18 (0.125)	529,800
C0125-02	3.18 (0.125)	255,750
C0125-03	3.18 (0.125)	134,150
C0125-04	3.18 (0.125)	71,150
C0125-05	3.18 (0.125)	204,500
C0125-06	3.18 (0.125)	1,125,300[b]
CP0125-01	3.18 (0.125)	1,060,950[b]
CP0125-02	3.18 (0.125)	722,000[b]
CPB0250-03	6.35 (0.25)	1,318,900[b]
CPB0250-04	6.35 (0.25)	1,318,900[b]
CPB0250-05	6.35 (0.25)	1,547,850[b]
CPB0250-06	6.35 (0.25)	1,547,850[b]
CP0065-01	1.59 (0.0625)	279,750
CP0065-02	1.59 (0.0625)	283,900
CP0065-03	1.59 (0.0625)	802,900
CP0065-04	1.59 (0.0625)	153,706
CP0065-05	1.59 (0.0625)	637,846
CPB0250-07	6.35 (0.25)	1,550,450[b]
CPB0250-08	6.35 (0.25)	1,550,450[b]
CPB0250-01	6.35 (0.25)	1,205,315
CPB0250-02	6.35 (0.25)	1,634,756[b]
CPB0125-01	3.18 (0.125)	1,725,900[b]
CPB0125-02	3.18 (0.125)	1,725,900[a]
CPB0125-03	3.18 (0.125)	1,564,300[b]
CPB0125-04	3.18 (0.125)	1,564,300[b]

[a]All tests were performed at a stress range of 138 MPa (20 ksi).
[b]Test was stopped without observed debonding after number of cycles exceeded infinite fatigue life.

with breather cloth and a resin pool (tested as part of this study) are designated by CPB, and the three specimens with chopped fiber overlays (also tested as part of this study) are designated by the letters CHP. A resin pool was created by leaving a gap of at least 13 mm (0.5 in.) between the edge of the overlay and the edge of the resin layer used to attach the overlay to the steel. A detailed step-by-step description of the fabrication process is given by Kaan (2008). The number in the designation of specimens with multilayered overlays represents the thickness of the bond layer in units of in. $\times 10^3$.

The term "run-out" is used in this paper in reference to specimens that achieved a large number of cycles, near to or exceeding the infinite fatigue-life threshold specified by the AASHTO fatigue design curves, after which testing was discontinued. In most instances reported in this paper, specimens that achieved run-out also exceeded the infinite fatigue-life threshold for the corresponding AASHTO fatigue-design category and stress range without developing observable fatigue cracks. The results show that, with one exception, all specimens with multilayered overlays that were bonded using breather cloth achieved run-out at very high stress ranges without failure of the bond layer. This is in direct contrast with the trials without breather cloth carried out by Kaan (2008). For example, a fatigue test reported by Kaan (2008) performed on a steel specimen with CFRP bonded to it without breather cloth cycled 1.33 million times before crack initiation; however, the CFRP overlays debonded six times during the test. Each time debonding occurred, the CFRP overlay was completely removed from the specimen and rebonded. The thickness of the resin layer was 3 mm (1/8 in.). Fatigue tests performed using breather cloth embedded in the resin bond layer of the same thickness [3 mm (1/8 in.)] sustained 3.3 million cycles without any observed debonding between the CFRP and steel. After 1.5 million cycles, the CFRP overlay was removed and the steel substrate was inspected for cracks. No cracks were discovered. In specimens without breather cloth the average fatigue life of the bond layer with a thickness of 2 mm (1/16 in.) was 431,000 cycles, whereas the average fatigue life for bond layers with a thickness of 3 mm (1/8 in.) was 240,000 cycles. The coefficients of variation were 0.64 and 0.74, respectively. The scatter of the results can be appreciated in Fig. 12. The fact that the trend opposes the results from the finite-element analyses, and the degree of scatter, were indicative that fabrication problems in the bond layer induced significant variability in the results and severely affected the fatigue-crack initiation life of the bond layer. A detailed description of the type of fabrication problems encountered and the effect of breather cloth on the quality of the bond layer is presented elsewhere (Alemdar et al. 2011).

Of the three specimens reinforced with chopped-fiber overlays, the best results were obtained with test CHP2, in which a layer of breather cloth was first saturated with the same resin used in the chopped-fiber composite, and later sprayed with the resin-fiber mix. Test CHP1, in which the chopped-fiber mix was sprayed directly on the steel surface, had very weak bond strength under fatigue loading. This was also the case for test CHP3, in which a layer of Hysol with embedded breather cloth was adhered to the steel before spraying with the resin-fiber mix. In this case, failure occurred at the interface between the Hysol® and the sprayed-fiber composite. Results from the sprayed-fiber specimens indicate that this method of fabrication of the overlay has merit as a repair technique, with the most promising results exhibited by the bond technique used in test CHP2. However, refinements to the bonding technique are still needed to achieve bond performance necessary to reach the infinite fatigue-life threshold of the welded connection.

Fatigue-Crack Initiation Life of the Welded Connections

The tests performed with breather cloth in the bond layer showed that by implementing this fabrication technique the bond layer could achieve run-out under very high applied-stress range. Having addressed the bond problem under fatigue loading, the remaining research problem was whether the reduction in stress demand afforded by the composite overlays would be sufficient to extend the fatigue life of the welded connections to the infinite range, as suggested by the results from the finite-element analysis. To address this question, two specimens were strengthened with CFRP overlays using breather cloth within the resin layer. The first, designated as TRI 06 in Tables 2 and 5, had been previously loaded with 1.6 million cycles without developing observable fatigue cracks (Kaan 2008). Testing conducted during the initial 1.6 million cycles included a resin layer 2-mm (1/16-in.) thick, without breather cloth. Subsequent testing performed on TRI 06 used a resin layer 6-mm (1/4-in.) thick with breather cloth embedded within the bond layer. The specimen was tested under fatigue loading with the same protocol described in Kaan (2008). After 1.55 million cycles, the test was stopped and the composite overlay removed to inspect the weld for crack initiation. No cracks were observed.

The second specimen, designated as TRI 07, was treated with a CFRP overlay and breather cloth and had not been loaded before this study. The thickness of the resin layer was 3 mm (⅛ in.) and it

Table 5. Experimental Results of Three-Point Bending Tests

Specimen designation	Stress range MPa (ksi)	Bond layer thickness mm (in.)	No. of cycles[a]	No. of cycles to crack initiation	Operator
TRI 02	137.9 (20.0)	0.76 (0.03)	900,000	N/A	Kaan (2008)
TRI 04	137.9 (20.0)	3.18 1/8 = 0.125	4,918,550[b]	N/A	Kaan (2008)-Alemdar[d]
TRI 05	137.9 (20.0)	6.35 1/4 = 0.25	1,634,756	N/A	Kaan (2008)
TRI 05	137.9 (20.0)	6.35 1/4 = 0.25	1,634,756	N/A	Kaan (2008)
TRI 06	137.9 (20.0)	1.59 1/16 = 0.0625	3,105,106	N/A	Kaan (2008)-Alemdar[d]
TRI 06	137.9 (20.0)	1.59 1/16 = 0.0625	3,105,106	N/A	Kaan (2008)-Alemdar[d]
TRI 07	137.9 (20.0)	3.18 1/8 = 0.125	3,290,200[c]	N/A	Alemdar[d]
TRI 07	137.9 (20.0)	3.18 1/8 = 0.125	3,290,200[c]	N/A	Alemdar[d]
TRI 08	137.9 (20.0)			355,450	Alemdar[d]
GRND 1	193.1 (28.0)			391,000	Alemdar[d]
GRND 2	193.1 (28.0)			1,200,000	Alemdar[d]
GRND 3	193.1 (28.0)			950,000	Alemdar[d]
GRND 4	193.1 (28.0)			600,000	Alemdar[d]
UIT 02	193.1 (28.0)			1,300,000	Vilhauer et al. (2012)
UIT 03	193.1 (28.0)			2,100,000	Vilhauer et al. (2012)
UIT 01	137.9 (20.0)		5,000,000	N/A	Vilhauer et al. (2012)
Cntrl_05	193.1 (28.0)			80,000	Vilhauer et al. (2012)
Cntrl_06	193.1 (28.0)			50,000	Vilhauer et al. (2012)
Cntrl_04	137.9 (20.0)			350,000	Vilhauer et al. (2012)

[a]Specimens that achieved runnout.
[b]After 1.3 mil cycles and at the end of the test overlays were removed to measure crack length.
[c]After 1.5 mil cycles and at the end of the test overlays were removed to inspect for the presence of cracks.
[d]F. Alemdar, unpublished data, 2011.

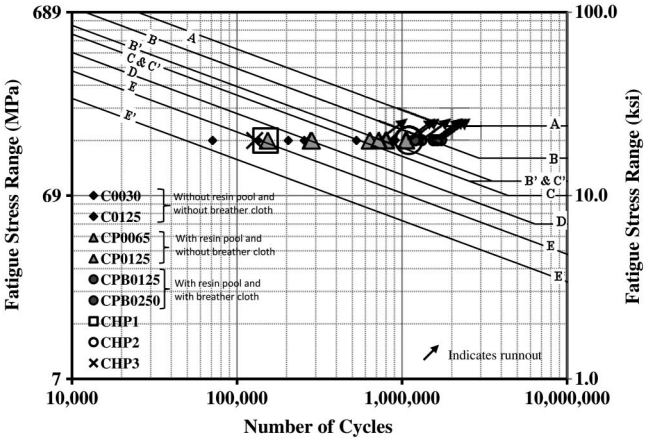

Fig. 12. Fatigue life of bond layer for various bonding techniques

had embedded breather cloth. This specimen was subjected to the fatigue-loading protocol for a total of 3.29 million cycles. After the first 1.50 million cycles, the test was paused and the overlays were removed to inspect for fatigue cracks. After inspection, the overlays were reattached and the specimen loaded until a total of 3.29 million cycles were reached. The final inspection showed that the specimen had not developed any detectable fatigue cracks.

To gauge the effectiveness of the CFRP overlay repair technique, results from specimens reinforced with composite overlays were compared with improvements in fatigue life associated with other repair techniques evaluated using the same type of specimens. Results are summarized in Table 5 and presented in Fig. 13. Specimens that were treated by smoothing of the welds are designated by GRND, specimens in which the welds were treated with UIT are designated by UIT, and control specimens are designated by Cntrl.

On average, control specimens tested at a stress range of 193 MPa (28 ksi) had a fatigue-crack initiation life of 65,000 cycles. Specimens with smoothed welds tested at the same stress range had an average fatigue life of 785,250 cycles with a coefficient of variation of 0.46. This weld treatment technique resulted in a very significant increase in fatigue life, on average raising the fatigue performance from AASHTO fatigue-design Category E' to AASHTO fatigue-design Category B. However, if the same statistical approach used to derive the AASHTO fatigue-design curves is followed, the high variance of the results would lead to a much more modest increase in fatigue category. Fig. 13 shows that treating the specimens with composite overlays or treating the weld with Ultrasonic Impact Treatment were equally effective, extending fatigue life to run-out in both instances.

Fatigue-Crack Propagation Life of the Welded Connections with CFRP Overlays

One of the specimens, designated as TRI 04, was previously tested by Kaan (2008) and developed a fatigue crack after 1.36 million cycles. This specimen was repaired with CFRP overlays with breather cloth embedded in the resin layer. The fatigue crack, detected using dye penetrant after testing by Kaan (2008), was approximately 2-mm (1/16-in.) long in the width direction. This pre cracked specimen was reinforced with CFRP overlays with a 6-mm (1/4-in.) thick resin layer and subjected to additional fatigue loading. After 1.3 million cycles into the additional testing, the CFRP overlays were removed to inspect for fatigue cracks. After inspection, the overlays were reattached and the specimen loaded until a total of 2.88 million cycles were reached. A caliper measurement taken during final inspection showed that the crack

J. Bridge Eng. 2012.17:420-431.

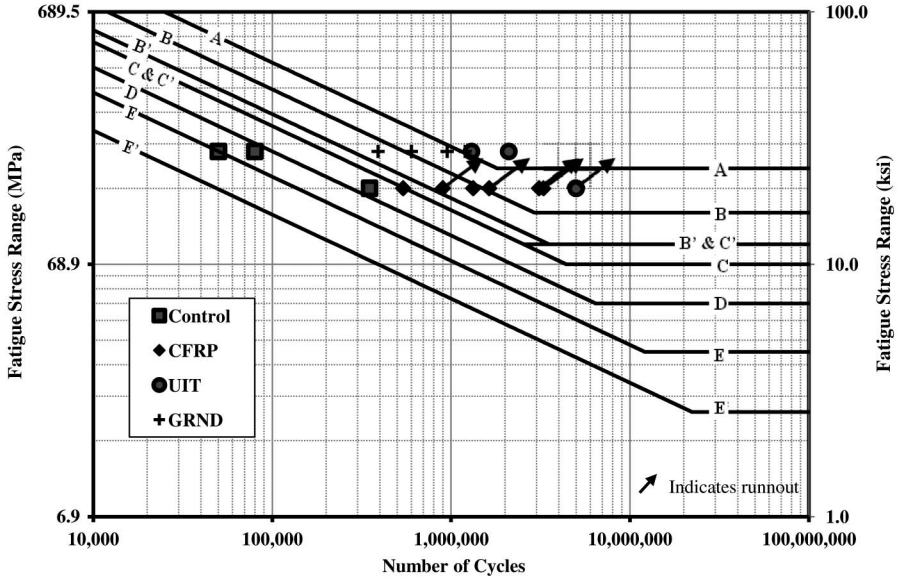

Fig. 13. Fatigue life of welded connections for various types of treatments

length was approximately the same, within the accuracy of the caliper.

It is meaningful to compare experimental results with theoretical fatigue-life estimates. Theoretical calculations of fatigue-crack propagation life were performed using two different underlying assumptions: (1) a surface crack in an infinite plate, and (2) an edge crack in a finite plate. The theoretical model based on the assumption of an edge crack in a finite plate (Cartwright et al. 1976) captured the known thickness and known width of the steel specimen. It assumed a semi-elliptical edge crack subjected to uniaxial tensile stress. These calculated values were compared with experimental measurements of crack length at a known number of fatigue cycles after crack initiation, as presented in Fig. 14. This theoretical calculation, based on the assumption of an edge crack in a finite plate, yielded the closest match to experimental results obtained by Vilhauer et al. (2012) using a control specimen. The experimental results obtained by Vilhauer, taken from a specimen subjected to a stress range of 193 MPa (28 ksi), are shown for reference in Fig. 14. Other theoretical models that were considered (e.g., surface crack in a finite plate) produced results that lay between those of the surface crack in an infinite plate and the edge crack in a finite plate. Therefore, for clarity, only the former and latter theoretical crack-growth computed values are presented in Fig. 14. Theoretical crack-propagation rates were examined at various stress ranges, with the aim of determining the actual stress range the welded connection was subjected to when CFRP overlays were bonded to the specimens. The experimental crack lengths measured in steel specimens retrofitted with CFRP overlays (shown in Fig. 14 as diamond symbols) were found in close agreement with the theoretical crack-growth estimates for a bare-steel specimen subjected to a 34.5 MPa (5 ksi) stress range. Therefore, this exercise suggests that a Category E' specimen with CFRP overlays bonded to it and tested at a stress range of 138 MPa (20 ksi) may be expected to perform similarly to an identical bare-steel specimen tested at a stress range of 34.5 MPa (5 ksi), suggesting a reduction of 80% in the stress demand, which is consistent with results from the finite-element analyses. Although negligible crack growth was observed after 2.88 million cycles, the estimated fatigue-crack

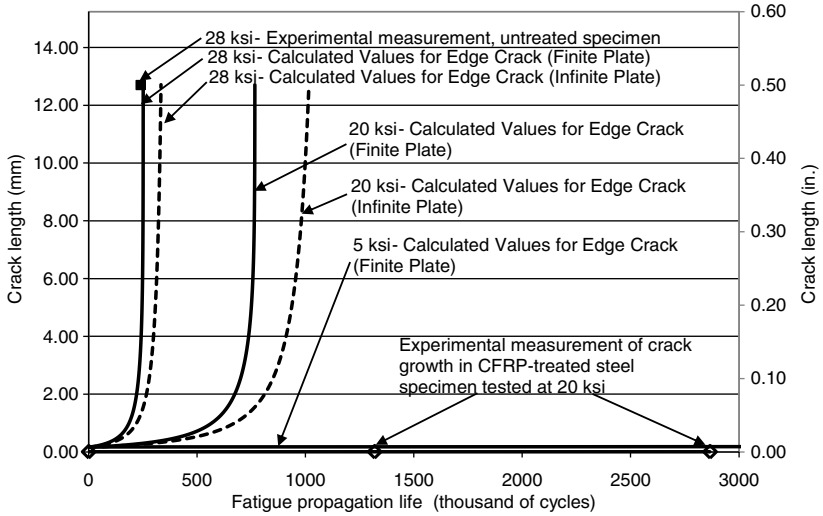

Fig. 14. Theoretical and experimental propagation life of untreated and CFRP-retrofitted three-point bending specimens

J. Bridge Eng. 2012.17:420-431.

propagation life of an untreated specimen subjected to a similar stress range was 766,000 cycles.

Conclusions

Several techniques exist that may be used to increase the fatigue-crack initiation life in welded connections. Options for reducing crack growth rate in welded connections are much more limited because of difficulties presented by complex geometry that often exist at fatigue-vulnerable connections. This study focused on the use of CFRP overlays to repair and strengthen welded connections of structural steel members. Using CFRP overlays was found to be highly effective both as a preventive measure to extend the fatigue-crack initiation life of welded connections and as a repair measure to reduce the stress demand in welded connections below the crack-propagation threshold. An improvement in fatigue-crack initiation life of at least 9 times was recorded for specimen TRI 06, and at least 9.5 times for specimen TRI 07, when compared with the fatigue-crack initiation life of untreated steel specimens tested at the same stress range. Composite overlays were as effective as other established repair methods such as ultrasonic impact treatment (UIT), which have been shown to provide significant improvements in fatigue-crack initiation life [14 times, reported by Vilhauer et al. (2012)].

The CFRP-retrofitted pre-cracked specimen sustained an additional total of 2.88 million cycles after crack initiation without any measurable crack growth. This test showed that the CFRP overlays were able to reduce the stress range at the critical point of the welded connection below the crack-propagation threshold.

Given the relatively simple bonding techniques employed, with the proper level of training, this repair technique is anticipated to be equally effective under field conditions, although some important considerations need to be addressed before it is practical to do so with confidence.

Acknowledgments

The authors are grateful for support from the Kansas Department of Transportation (KDOT) and the University of Kansas Transportation Research Institute (KU TRI). The authors would also like to acknowledge support provided through Pooled Fund Study TPF-5(189), which includes the following participating state DOTs: Kansas, California, Iowa, Illinois, New Jersey, New York, Oregon, Pennsylvania, Tennessee, Wisconsin, and Wyoming, as well as the Federal Highway Administration.

References

AASHTO. (2004). *Bridge design specifications*, Washington, DC.

Albrecht, P., and Lenwari, A. (2007). "Fatigue-proofing cover plates." *J. Bridge Eng.*, 12(3), 275–283.

Alemdar, F., Matamoros, A., Bennett, C., Barrett-Gonzalez, R., and Rolfe, S. (2011). "Improved method for bonding CFRP overlays to steel for fatigue repair." *Proc., ASCE/SEI Structures Congress*, ASCE, Reston, VA.

ASTM. (2000). "Standard test method for tensile properties of polymer matrix composite materials." *3039/D 3039M*, West Conshohocken, PA.

Barsom, J. M., and Rolfe, S. T. (1999). *Fracture and fatigue control in structures: Applications of fracture mechanics*, 3rd Ed., ASTM International, West Conshohocken, PA.

Cartwright, D. J., and Rooke, D. P. (1976). "The compounding method applied to cracks in stiffened sheets." *Eng. Fract. Mech.*, 8(3), 567–573.

Kaan, B. (2008). Fatigue enhancement of Category E' details in steel bridge girder using CFRP materials." M.S. thesis, Dept. of Civil, Architectural and Environmental Engineering, Univ. of Kansas, Lawrence, KS.

Nakamura, H., Jiang, W., Suzuki, H., Maeda, K., and Irube, T. (2009). "Experimental study on repair of fatigue cracks at welded web gusset joint using CFRP strips." *Thin-Walled Struct.*, 47(10), 1059–1068.

Petri, B. (2008). "Finite element analysis of steel welded coverplate including composite doublers." M.S. thesis, Dept. of Civil, Architectural and Environmental Engineering, Univ. of Kansas, Lawrence, KS.

Sabelkin, V., Mall, S., Hansen, M. A., Vandawaker, R. M., and Derris, M. (2007). "Investigation into cracked aluminum plate repaired with bonded composite patch." *Compos. Struct.*, 79(1), 55–66.

Simulia (2008). ABAQUS FEA Version 6.8.2. Providence, RI ⟨http://www.simulia.com⟩.

Schubbe, J. J., and Mall, S. (1999). "Investigation of a cracked thick aluminum panel repaired with a bonded composite patch." *Eng. Fract. Mech.*, 63(3), 305–323.

Tavakkolizadeh, M., and Saadatmanesh, H. (2003). "Fatigue strength of steel girders strengthened with carbon fiber reinforced polymer patch." *J. Struct. Eng.*, 129(2),186–196.

Vilhauer, B., Bennett, C., Matamoros, A., and Rolfe, S. (2012). "Fatigue behavior of welded coverplates treated with ultrasonic impact treatment and bolting." *Eng. Struct.*, 34, 163–172.